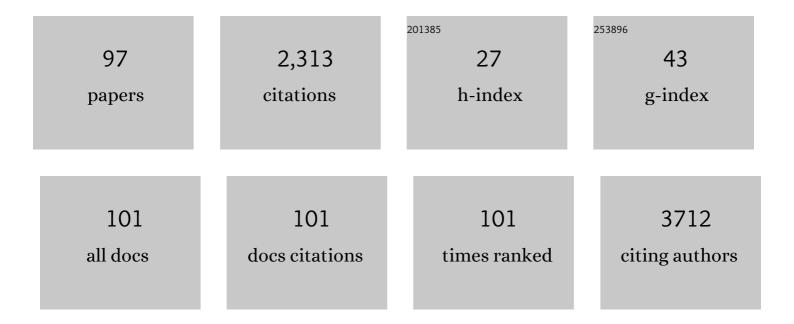
List of Publications by Year in descending order

Source: https://exaly.com/author-pdf/1885561/publications.pdf Version: 2024-02-01



#	Article	IF	CITATIONS
1	Photoinduced iodide repulsion and halides-demixing in layered perovskites. Materials Today Nano, 2022, 18, 100197.	2.3	5
2	Highly enhanced ferroelectricity in HfO ₂ -based ferroelectric thin film by light ion bombardment. Science, 2022, 376, 731-738.	6.0	58
3	Nanomechanical sampling of material for nanoscale mass spectrometry chemical analysis. Analytical and Bioanalytical Chemistry, 2021, 413, 2747-2754.	1.9	Ο
4	Direct Observation of Photoinduced Ion Migration in Lead Halide Perovskites. Advanced Functional Materials, 2021, 31, 2008777.	7.8	41
5	Enhancing hyperspectral EELS analysis of complex plasmonic nanostructures with pan-sharpening. Journal of Chemical Physics, 2021, 154, 014202.	1.2	5
6	Quantitative Measurement of Li-Ion Concentration and Diffusivity in Solid-State Electrolyte. ACS Applied Energy Materials, 2021, 4, 784-790.	2.5	6
7	Correlating Crystallographic Orientation and Ferroic Properties of Twin Domains in Metal Halide Perovskites. ACS Nano, 2021, 15, 7139-7148.	7.3	14
8	Strain in Metal Halide Perovskites: The Critical Role of A-Site Cation. ACS Applied Energy Materials, 2021, 4, 2068-2072.	2.5	14
9	Role of Decomposition Product Ions in Hysteretic Behavior of Metal Halide Perovskite. ACS Nano, 2021, 15, 9017-9026.	7.3	13
10	Ferroelectric and Charge Transport Properties in Strain-Engineered Two-Dimensional Lead Iodide Perovskites. Chemistry of Materials, 2021, 33, 4077-4088.	3.2	10
11	Ferroic Halide Perovskite Optoelectronics. Advanced Functional Materials, 2021, 31, 2102793.	7.8	23
12	Helium Ion Microscopy with Secondary Ion Mass Spectrometry for Nanoscale Chemical Imaging and Analysis of Polyolefins. ACS Applied Polymer Materials, 2021, 3, 3478-3484.	2.0	2
13	Building an edge computing infrastructure for rapid multi-dimensional electron microscopy. Microscopy and Microanalysis, 2021, 27, 56-57.	0.2	2
14	Lossless Deep Image Compression at the Edge for 3D Electron Microscopy. Microscopy and Microanalysis, 2021, 27, 472-473.	0.2	1
15	Beyond NMF: Advanced Signal Processing and Machine Learning Methodologies for Hyperspectral Analysis in EELS. Microscopy and Microanalysis, 2021, 27, 322-324.	0.2	3
16	Ferroic Halide Perovskite Optoelectronics (Adv. Funct. Mater. 36/2021). Advanced Functional Materials, 2021, 31, 2170263.	7.8	1
17	Nanoscale friction of CVD single-layer MoS2 with controlled defect formation. Surfaces and Interfaces, 2021, 26, 101437.	1.5	5
18	Unraveling the hysteretic behavior at double cations-double halides perovskite - electrode interfaces. Nano Energy, 2021, 89, 106428.	8.2	11

#	Article	IF	CITATIONS
19	Microstructural Evaluation of Phase Instability in Large Bandgap Metal Halide Perovskites. ACS Nano, 2021, 15, 20391-20402.	7.3	8
20	Structures of Partially Fluorinated Bottlebrush Polymers in Thin Films. ACS Applied Polymer Materials, 2020, 2, 209-219.	2.0	7
21	Nanoscale Mass Spectrometry Multimodal Imaging <i>via</i> Tip-Enhanced Photothermal Desorption. ACS Nano, 2020, 14, 16791-16802.	7.3	6
22	Hysteretic Ion Migration and Remanent Field in Metal Halide Perovskites. Advanced Science, 2020, 7, 2001176.	5.6	29
23	Operando Imaging of Ion Migration in Metal Halide Perovskites. Microscopy and Microanalysis, 2020, 26, 2046-2048.	0.2	0
24	In situ multimodal imaging for nanoscale visualization of tribofilm formation. Journal of Applied Physics, 2020, 127, 154303.	1.1	4
25	Direct Write of 3D Nanoscale Mesh Objects with Platinum Precursor via Focused Helium Ion Beam Induced Deposition. Micromachines, 2020, 11, 527.	1.4	15
26	Secondary Ion Mass Spectrometry (SIMS) for Chemical Characterization of Metal Halide Perovskites. Advanced Functional Materials, 2020, 30, 2002201.	7.8	29
27	Toward nanoscale molecular mass spectrometry imaging via physically constrained machine learning on co-registered multimodal data. Npj Computational Materials, 2020, 6, .	3.5	15
28	Correlated Electrical and Chemical Nanoscale Properties in Potassiumâ€Passivated, Triple ation Perovskite Solar Cells. Advanced Materials Interfaces, 2020, 7, 2000515.	1.9	4
29	Exploration of Electrochemical Reactions at Organic–Inorganic Halide Perovskite Interfaces via Machine Learning in In Situ Timeâ€ofâ€Flight Secondary Ion Mass Spectrometry. Advanced Functional Materials, 2020, 30, 2001995.	7.8	30
30	Machine learning-based multidomain processing for texture-based image segmentation and analysis. Applied Physics Letters, 2020, 116, .	1.5	19
31	Twin domains modulate light-matter interactions in metal halide perovskites. APL Materials, 2020, 8, .	2.2	17
32	Strain–Chemical Gradient and Polarization in Metal Halide Perovskites. Advanced Electronic Materials, 2020, 6, 1901235.	2.6	19
33	Tuning spin-orbit coupling towards enhancing photocurrent in hybrid organic-inorganic perovskites by using mixed organic cations. Organic Electronics, 2020, 81, 105671.	1.4	10
34	Spectral Map Reconstruction Using Pan-Sharpening Algorithm: Enhancing Chemical Imaging with AFM-IR. Microscopy and Microanalysis, 2019, 25, 1024-1025.	0.2	2
35	Multi-Model Imaging of Local Chemistry and Ferroic Properties of Hybrid Organic-Inorganic Perovskites. Microscopy and Microanalysis, 2019, 25, 2076-2077.	0.2	3
36	Non-conventional mechanism of ferroelectric fatigue via cation migration. Nature Communications, 2019, 10, 3064.	5.8	23

#	Article	IF	CITATIONS
37	Investigation of Electrode Electrochemical Reactions in CH ₃ NH ₃ PbBr ₃ Perovskite Singleâ€Crystal Fieldâ€Effect Transistors. Advanced Materials, 2019, 31, e1902618.	11.1	74
38	Quantitative Electromechanical Atomic Force Microscopy. ACS Nano, 2019, 13, 8055-8066.	7.3	84
39	Ferroic twin domains in metal halide perovskites. MRS Advances, 2019, 4, 2817-2830.	0.5	7
40	Helium Ion Microscopy Imaging of Bottlebrush Copolymers. Microscopy and Microanalysis, 2019, 25, 908-909.	0.2	0
41	Twoâ€Photon Upâ€Conversion Photoluminescence Realized through Spatially Extended Gap States in Quasiâ€2D Perovskite Films. Advanced Materials, 2019, 31, 1901240.	11.1	23
42	Lightâ€Ferroic Interaction in Hybrid Organic–Inorganic Perovskites. Advanced Optical Materials, 2019, 7, 1901451.	3.6	24
43	Surface Analysis of Polymers using Helium Ion Microscopy Coupled with Secondary Ion Mass Spectrometry (HIM-SIMS). Microscopy and Microanalysis, 2019, 25, 868-869.	0.2	1
44	High Resolution Multimodal Chemical Imaging Platform for Organics and Inorganics. Analytical Chemistry, 2019, 91, 12142-12148.	3.2	16
45	Multimodal Chemical Imaging for Linking Adhesion with Local Chemistry in Agrochemical Multicomponent Polymeric Coatings. Analytical Chemistry, 2019, 91, 2791-2796.	3.2	8
46	Deep data analytics for genetic engineering of diatoms linking genotype to phenotype via machine learning. Npj Computational Materials, 2019, 5, .	3.5	16
47	Application of pan-sharpening algorithm for correlative multimodal imaging using AFM-IR. Npj Computational Materials, 2019, 5, .	3.5	9
48	Deep neural networks for understanding noisy data applied to physical property extraction in scanning probe microscopy. Npj Computational Materials, 2019, 5, .	3.5	43
49	Environmental Gating and Galvanic Effects in Single Crystals of Organic–Inorganic Halide Perovskites. ACS Applied Materials & Interfaces, 2019, 11, 14722-14733.	4.0	14
50	Reply to: On the ferroelectricity of CH3NH3PbI3 perovskites. Nature Materials, 2019, 18, 1051-1053.	13.3	21
51	Subtractive fabrication of ferroelectric thin films with precisely controlled thickness. Nanotechnology, 2018, 29, 155302.	1.3	7
52	Multi-purposed Ar gas cluster ion beam processing for graphene engineering. Carbon, 2018, 131, 142-148.	5.4	18
53	Chemical Phenomena of Atomic Force Microscopy Scanning. Analytical Chemistry, 2018, 90, 3475-3481.	3.2	20
54	Photothermoelastic contrast in nanoscale infrared spectroscopy. Applied Physics Letters, 2018, 112, 033105.	1.5	8

#	Article	IF	CITATIONS
55	Helium Ion Microscopy for Imaging and Quantifying Porosity at the Nanoscale. Analytical Chemistry, 2018, 90, 1370-1375.	3.2	17
56	Liquid Cell Crystallization and In-situ Imaging of Thiamethoxam by Helium Ion Microscopy. Microscopy and Microanalysis, 2018, 24, 330-331.	0.2	0
57	Correlated Materials Characterization <i>via</i> Multimodal Chemical and Functional Imaging. ACS Nano, 2018, 12, 11798-11818.	7.3	28
58	<i>In situ</i> liquid cell crystallization and imaging of thiamethoxam by helium ion microscopy. Journal of Vacuum Science and Technology B:Nanotechnology and Microelectronics, 2018, 36, .	0.6	3
59	Nanoscale Electrochemical Phenomena of Polarization Switching in Ferroelectrics. ACS Applied Materials & Interfaces, 2018, 10, 38217-38222.	4.0	18
60	Molecular reorganization in bulk bottlebrush polymers: direct observation <i>via</i> nanoscale imaging. Nanoscale, 2018, 10, 18001-18009.	2.8	14
61	3D Nanostructures Grown via Focused Helium Ion Beam Induced Deposition. Microscopy and Microanalysis, 2018, 24, 332-333.	0.2	1
62	Elasticity Modulation Due to Polarization Reversal and Ionic Motion in the Ferroelectric Superionic Conductor KTiOPO ₄ . ACS Applied Materials & Interfaces, 2018, 10, 32298-32303.	4.0	11
63	Surface Chemistry Controls Anomalous Ferroelectric Behavior in Lithium Niobate. ACS Applied Materials & Interfaces, 2018, 10, 29153-29160.	4.0	20
64	Chemical nature of ferroelastic twin domains in CH3NH3PbI3 perovskite. Nature Materials, 2018, 17, 1013-1019.	13.3	183
65	Dynamic behavior of CH3NH3PbI3 perovskite twin domains. Applied Physics Letters, 2018, 113, .	1.5	27
66	Time resolved surface photovoltage measurements using a big data capture approach to KPFM. Nanotechnology, 2018, 29, 445703.	1.3	36
67	Nanoscale Control of Oxygen Defects and Metal–Insulator Transition in Epitaxial Vanadium Dioxides. ACS Nano, 2018, 12, 7159-7166.	7.3	41
68	Graphene milling dynamics during helium ion beam irradiation. Carbon, 2018, 138, 277-282.	5.4	18
69	Ion Migration Studies in Exfoliated 2D Molybdenum Oxide via Ionic Liquid Gating for Neuromorphic Device Applications. ACS Applied Materials & Interfaces, 2018, 10, 22623-22631.	4.0	12
70	Improved spatial resolution for spot sampling in thermal desorption atomic force microscopy – mass spectrometry via rapid heating functions. Nanoscale, 2017, 9, 5708-5717.	2.8	9
71	Enhancing Ion Migration in Grain Boundaries of Hybrid Organic–Inorganic Perovskites by Chlorine. Advanced Functional Materials, 2017, 27, 1700749.	7.8	74
72	Buckling Instabilities in Polymer Brush Surfaces via Postpolymerization Modification. Macromolecules, 2017, 50, 8670-8677.	2.2	15

#	Article	IF	CITATIONS
73	Building with ions: towards direct write of platinum nanostructures using in situ liquid cell helium ion microscopy. Nanoscale, 2017, 9, 12949-12956.	2.8	8
74	Noble gas ion beams in materials science for future applications and devices. MRS Bulletin, 2017, 42, 660-666.	1.7	23
75	Automated Interpretation and Extraction of Topographic Information from Time of Flight Secondary Ion Mass Spectrometry Data. Scientific Reports, 2017, 7, 17099.	1.6	21
76	Chemical Changes in Layered Ferroelectric Semiconductors Induced by Helium Ion Beam. Scientific Reports, 2017, 7, 16619.	1.6	3
77	Metal/Ion Interactions Induced p–i–n Junction in Methylammonium Lead Triiodide Perovskite Single Crystals. Journal of the American Chemical Society, 2017, 139, 17285-17288.	6.6	32
78	Engineering the thermal conductivity along an individual silicon nanowire by selective helium ion irradiation. Nature Communications, 2017, 8, 15919.	5.8	65
79	Building with Ions in the Helium Ion Microscope. Microscopy and Microanalysis, 2017, 23, 260-261.	0.2	0
80	Building with Ions: Development of In-situ Liquid Cell Microscopy for the Helium Ion Microscope Microscopy and Microanalysis, 2016, 22, 754-755.	0.2	0
81	Directing Matter: Toward Atomic-Scale 3D Nanofabrication. ACS Nano, 2016, 10, 5600-5618.	7.3	99
82	Polarization Control via He-Ion Beam Induced Nanofabrication in Layered Ferroelectric Semiconductors. ACS Applied Materials & amp; Interfaces, 2016, 8, 7349-7355.	4.0	19
83	Chemical State Evolution in Ferroelectric Films during Tip-Induced Polarization and Electroresistive Switching. ACS Applied Materials & Interfaces, 2016, 8, 29588-29593.	4.0	33
84	Atomistic-Scale Simulations of Defect Formation in Graphene under Noble Gas Ion Irradiation. ACS Nano, 2016, 10, 8376-8384.	7.3	113
85	Nanoforging Single Layer MoSe2 Through Defect Engineering with Focused Helium Ion Beams. Scientific Reports, 2016, 6, 30481.	1.6	82
86	lonic Liquid Activation of Amorphous Metalâ€Oxide Semiconductors for Flexible Transparent Electronic Devices. Advanced Functional Materials, 2016, 26, 2820-2825.	7.8	46
87	Deciphering Halogen Competition in Organometallic Halide Perovskite Growth. Journal of the American Chemical Society, 2016, 138, 5028-5035.	6.6	92
88	Graphene engineering by neon ion beams. Nanotechnology, 2016, 27, 125302.	1.3	21
89	Co-registered Topographical, Band Excitation Nanomechanical, and Mass Spectral Imaging Using a Combined Atomic Force Microscopy/Mass Spectrometry Platform. ACS Nano, 2015, 9, 4260-4269.	7.3	31
90	Atomic Force Microscope Controlled Topographical Imaging and Proximal Probe Thermal Desorption/Ionization Mass Spectrometry Imaging. Analytical Chemistry, 2014, 86, 1083-1090.	3.2	44

#	Article	IF	CITATIONS
91	Controlled-Resonant Surface Tapping-Mode Scanning Probe Electrospray Ionization Mass Spectrometry Imaging. Analytical Chemistry, 2014, 86, 3146-3152.	3.2	17
92	Laser microdissection and atmospheric pressure chemical ionization mass spectrometry coupled for multimodal imaging. Rapid Communications in Mass Spectrometry, 2013, 27, 1429-1436.	0.7	33
93	Molecular Surface Sampling and Chemical Imaging using Proximal Probe Thermal Desorption/Secondary Ionization Mass Spectrometry. Analytical Chemistry, 2011, 83, 598-603.	3.2	36
94	Combined Atomic Force Microscope-Based Topographical Imaging and Nanometer-Scale Resolved Proximal Probe Thermal Desorption/Electrospray Ionization–Mass Spectrometry. ACS Nano, 2011, 5, 5526-5531.	7.3	47
95	Thinâ€layer chromatography and mass spectrometry coupled using proximal probe thermal desorption with electrospray or atmospheric pressure chemical ionization. Rapid Communications in Mass Spectrometry, 2010, 24, 1721-1729.	0.7	34
96	Combined chemical and topographic imaging at atmospheric pressure via microprobe laser desorption/ionization mass spectrometry–atomic force microscopy. Rapid Communications in Mass Spectrometry, 2009, 23, 3781-3786.	0.7	36
97	Light–ferroelectric interaction in two-dimensional lead iodide perovskites. Journal of Materials Chemistry A, 0, , .	5.2	1